Orientationally ordered phase produced by fully antinematic interactions: A simulation study

Silvano Romano*
Dipartimento di Fisica "A. Volta," Università di Pavia, Via A. Bassi 6, I-27100 Pavia, Italy

Giovanni De Matteis†
Dipartimento di Matematica "F. Casorati," Università di Pavia, Via Ferrata 1, I-27100 Pavia, Italy

(Received 10 December 2010; revised manuscript received 22 April 2011; published 8 July 2011)

We consider here a classical model, consisting of D_{2h} symmetric particles, whose centers of mass are associated with a three-dimensional simple-cubic lattice; the pair potential is isotropic in orientation space, and restricted to nearest neighbors. Two orthonormal triads define orientations of a pair of interacting particles; the simplest potential models proposed in the literature can be written as a linear combination involving the squares of the scalar products between corresponding unit vectors only, thus depending on three parameters, and making the interaction model rather versatile. A coupling constant with negative sign tends to keep the two interacting unit vectors parallel to each other, whereas a positive sign tends to keep them mutually orthogonal (antinematic coupling). We address here a special, extreme case of the above family, involving only antinematic couplings: more precisely, three antinematic terms whose coefficients are set to a common *positive value* (hence the name PPP model). The model under investigation produces a doubly degenerate pair ground state; the nearest-neighbor range of the interaction and the bipartite character of the lattice can propagate the pair ground state and increase the overall degeneracy, but without producing frustration. The model was investigated by a simplified molecular field treatment as well as by Monte Carlo simulation, whose results suggested a second-order transition to a low-temperature biaxially ordered phase; ground-state configurations producing orientational order have been selected by thermal fluctuations. The molecular field treatment also predicted a continuous transition, and was found to overestimate the transition temperature by a factor 2.

DOI: 10.1103/PhysRevE.84.011703 PACS number(s): 61.30.Cz

I. INTRODUCTION

Over the decades, the prediction of new possible phases (i.e., new types of structural order) often resulting from less usual microscopic interaction models, or just proposed as logical far-fetched possibilities [1,2], has emerged as an important aspect in liquid crystal research: The theoretical investigation has usually been worked out at various levels of approximation, and the search for experimental evidence of their realizations has often turned out to be a difficult and challenging task.

To quote one smectic example, let us mention that experimental evidence of triclinic fluid order (SmCPG phase) [1] has recently been found in a single, isolated fluid smectic liquid crystal layer, freely suspended in air [2], and resulting from suitable bent-core molecules [3].[1] Moreover, various phases involving no positional order and only a rotational one have been predicted so far: A detailed symmetry classification of these "unconventional" nematic phases, associated with the onset of either one tensor of rank different from two or of several combined tensors, has recently been carried out by Mettout [4–6], also in connection with bent-core mesogens [3,7].

Another case involves the possible existence of cubatic orientational order (i.e., along three mutually orthogonal axes): It had been investigated theoretically [8], and explicitly predicted in some specific cases, involving both hard-core [9–16] and continuous interaction models [17]; no experimental realizations of a cubatic phase are known for the time being.

Nematic phases are usually apolar and uniaxial, although the constituent molecules possess a lower symmetry; on the one hand, based on this observation, both theoretical treatments and interpretations of experimental results have often been simplified from the start by assuming that nematogenic molecules possess *uniaxial* ($D_{\infty h}$) symmetry. On the other hand, starting in the 1970s [18], a by now quite substantial amount of theoretical work had investigated the possible effects of molecular deviation from uniaxial symmetry [molecular biaxiality (MB)] on the resulting nematic order. Already by the end of the past century, approximate analytical theories such as molecular field (MF) or Landau treatments, and later simulation studies had shown that single-component models consisting of molecules possessing D_{2h} symmetry, and interacting by various appropriate continuous or hard-core

*Silvano.Romano@pv.infn.it
†giovanni.dematteis@unipv.it

[1] In Ref. [1], pages 275–277, de Gennes proposed the "rather far fetched possibility" of a tilted apolar smectic C phase, consisting of biaxial molecules, where the macroscopic second–rank ordering tensor is biaxial and its eigenframe bears no simple relationship with the layers (i.e., none of its three eigenvectors is either parallel or orthogonal to the layers); its layers would only possess inversion symmetry, and thus belong to the point symmetry class C_i; this was labelled SmCG phase (G for generic) [1,2]; notice also the footnote on page 275, explicitly excluding from the discussion both ferro– and antiferro–electric smectics, not known at that time. Actually, experimental realizations were later obtained (see Ref. [2] and others quoted therein), and it was also found that they can consist of suitable polar bent–core molecules, so that, in orientational terms, the phase symmetry may be even lower (C_1); these were called SmCGP phases (P for polar).

potentials, can produce a biaxial phase; a more extensive treatment and a more detailed bibliography can be found, for example, in Refs. [19,20]; a review on computer simulation studies of (thermotropic) biaxial nematic liquid crystals has recently been published [21].

As for experimental realizations, a biaxial phase had been discovered in a lyotropic system in 1980 [22]; since 1986, and until approximately 2003, there had been numerous reports of thermotropic biaxiality in low-molecular weight compounds, many of which were later called into question (see, e.g., Ref. [23]). Better experimental evidence was claimed since 2004, and by now for a few classes of compounds, such as polar bent-core molecules (see, e.g., Ref. [24], and also Ref. [25] about alternative interpretations), and organosiloxane tetrapodes or their counterparts with a germanium core (see, e.g., Refs. [26,27]); they have been investigated by various techniques, and biaxial order parameters have been measured in a few cases [28] (see also Refs. [21,25,29–31] for a thorough discussion and a more detailed bibliography). Here we limit ourselves to mention a few aspects which have been recently addressed. On the one hand, an alternative picture of biaxial nematic order [21,32–34] has been proposed, based on the idea of biaxial domains reoriented by surface anchoring or external fields; on the other hand, it has been pointed out that biaxial nematics need not possess the usually assumed D_{2h} symmetry, but a lower C_{2h} one is also appropriate [33,35–38].

Interest in biaxial nematics is also connected with their possible applications, for example, in displays [21,39–43]: Orientation of the secondary director in response to external perturbations is expected to be significantly faster than for the primary one.

Another theoretical possibility whose experimental realizations have actively been looked for involves polar nematic behavior in low molecular mass thermotropic mesogens [4–6,21,37,44,45]. Such materials are also expected to exhibit fast and easy response to external electric fields.

Over the decades, a rather simple, continuous, biaxial mesogenic model had been proposed [Eq. (4) in the following section] and investigated through contributions by a number of authors; we propose to label it *generalized Straley* (gS) model. On the other hand, various aspects of it, such as possible simplifications, additional symmetry, and versatility, have emerged over the last 5–10 years. Starting a few years ago (i.e., simultaneously with and independently of new experimental findings), a renewed theoretical study of the model and of its possible variants was started by Durand, Sonnet, and Virga (DSV) [46], and continued by them as well as other authors (see Refs. [47–51] and also the following section). The new proposed models, or, more precisely, the effect of new parameter choices in the gS model, were studied by MF (refined by a rigorous generalization of the minimax procedure where appropriate [48,51]), as well as by Monte Carlo simulation (MC) in the simple-cubic lattice-model version [19,52,53], and, in some cases, by two-site cluster (TSC) theory [54]. Moreover, very recently and motivated by the new experimental facts, the single-tensor Landau-deGennes theory of biaxial nematics has been carefully re-examined in Refs. [55,56] and a double-tensor Landau theory has been put forward and studied in Refs. [5,57].

The named potential models involve three independent parameters, and the above analysis showed that they are rather versatile (i.e., capable of producing both biaxial and purely uniaxial order in their ground states, and hence low-temperature phases). For example, last year, some other mesogenic lattice models, involving suitable antinematic terms in a pair potential of this type, had been proposed and analyzed in Ref. [58]; they were found to produce only uniaxial order in the low-temperature phase, and, in some cases, showed evidence of a continuous ordering transition.

Thus, we are considering here an extreme case where only antinematic couplings survive, tending to produce mutual perpendicular orientations of the interacting moieties, and defining a D_{2h}–symmetric extension of the Kohring-Shrock model [see Eq. (2) below].

In its simplest version, the well-known Lebwohl-Lasher (LL) lattice model [59,60] involves uniaxial ($D_{\infty h}$-symmetric) particles associated with the nodes of a simple-cubic lattice $\mathbb{Z}^3$, interacting via a pair potential restricted to nearest neighbors, and of the form,

$$\Phi = -\epsilon P_2(\mathbf{s}_\lambda \cdot \mathbf{s}_\mu). \tag{1}$$

Here, λ labels a lattice node, with coordinate vector $\mathbf{x}_\lambda$, and the unit vector $\mathbf{s}_\lambda$ defines orientation of the particle associated with the named node; $P_2(\ldots)$ denotes the second-order Legendre polynomial, and ϵ is a positive constant setting temperature and energy scales (i.e., $T^* = k_B T/\epsilon$).

Some years after the original papers by LL, Kohring and Shrock (KS) [61] proposed and studied the *antinematic* counterpart of the model, on the same lattice, and defined by

$$\Phi = +\epsilon P_2(\mathbf{s}_\lambda \cdot \mathbf{s}_\mu), \tag{2}$$

where the interaction favors mutual orthogonal (rather than parallel) orientation of pairs of nearest-neighboring particles; its ground state corresponds to a highly degenerate but nonfrustrated state (see also the following section). The intention of the named authors was not to provide an alternative model for uniaxial nematic liquid crystals, but rather to conceive a valuable model serving as a tool to address the fundamental statistical mechanical question of the effect of ground-state disorder without frustration [61]. KS carried out Monte Carlo calculations, and found evidence of a continuous ordering transition at finite temperature; the model was further investigated in Ref. [62] and a more detailed study took place in Ref. [63].

The present paper is organized as follows. In Sec. II the gS potential model is presented and the special case under investigation here is analyzed in greater detail, especially in its connection with the KS model. In Sec. III a simplified MF approximation is proposed and worked out. MC simulation aspects are addressed in Sec. IV, and the obtained results are presented in Sec. V. Finally, Sec. VI reports a summary and an outline of future research directions, and further mathematical details of the MF treatment are presented in Appendix A.

II. PAIR POTENTIALS AND GROUND STATES

It will prove convenient to start this section by recalling the possible ground-state configurations for the KS model [61,62];

let the three orthogonal unit vectors $\{\mathbf{e}_k, k = 1,2,3\}$ define an arbitrary Cartesian frame (which can, in this case, be taken as defined by the lattice axes, without any loss of generality). The lattice $\mathbb{Z}^3$ is bipartite: In other words, for each lattice site λ, let t_λ denote the sum of its three coordinates, so that site parity can be defined via the parity of the corresponding t_λ; then all nearest neighbors of a given lattice site have opposite parity, all next-nearest-neighbors have the same parity, and so on. The lattice thus results from two interpenetrating sublattices, composed of all even- or all odd-parity sites, respectively (even and odd sublattices, for short); moreover the interaction is restricted to nearest neighbors, thus between pairs of lattice sites possessing opposite parities. This combination of bipartite lattice and nearest-neighbor interaction entails that two different particles (or lattice sites) interacting with a third one never interact with each other (the uncoupling condition, for short).

Let us first remark that the pair ground state for the KS model possesses continuous degeneracy. One can, therefore, define a continuously degenerate overall ground state, by requesting that all particles associated with lattice sites of one parity point along a common direction, whereas particles on the other sublattice are randomly oriented perpendicular to the same direction, say $\mathbf{s}_\lambda = \pm\mathbf{e}_3$ for even-parity sites, and $\mathbf{s}_\lambda = \cos\phi_\lambda \mathbf{e}_1 + \sin\phi_\lambda \mathbf{e}_2$ for odd-parity sites, where the continuous random variables ϕ_λ associated with lattice sites λ are mutually independent; this set of configurations will be referred to as CC.

Upon averaging over CC (i.e., over the angles ϕ_λ), one would find uniaxial nematic order, the value 1/4 for the overall second-rank order parameter $\langle P_2\rangle$, and the value 11/16 for the overall fourth-rank order parameter $\langle P_4\rangle$ (see Refs. [60,64–66]), respectively. On the other hand, one can also consider discretized orientations of the individual particles, and define the set DA (D for discrete) of all overall ground-state configurations where each unit vector $\mathbf{s}_\lambda$ points along one of the three $\pm\mathbf{e}_k$ [the $\pm$ sign, allowing for particle symmetry, will be omitted in the following Eqs. (11), (15), and (16) for simplicity of notation], of course, while being orthogonal to its nearest neighbors; a subset of DA, to be called DB, is obtained by requesting that all particles associated with lattice sites of one parity point along a common direction (one of the three $\pm\mathbf{e}_k$), whereas particles associated with lattice sites of the opposite parity point along the two other available directions. In turn, DB contains a subset (to be called DC) where the other sublattice is occupied by particles in the two other possible orientations, and *with equal populations*. Notice that [61] DA also contains a subset of periodic configurations with period 3 (to be called D3), where the orientation of the particle sitting at the lattice site λ is defined in terms of the value mod $(t_\lambda,3)$, for example, by $\mathbf{e}_I, I = 1 + \mathrm{mod}\,(t_\lambda,3)$.

Upon averaging over all configurations in DA, second-rank orientational order would vanish, whereas fourth-rank order would survive, with the value $\langle P_4\rangle_{DA} = 7/12$ for the corresponding order parameter.

Simulation studies had shown [61,62] that, at sufficiently low but finite temperatures, only the above continuous degeneracy matters (i.e., only configurations belonging to or close to CC are selected by thermal fluctuations) as to be expected; ordering by entropic effect (or "by disorder"; see, e.g., Refs. [67–69]) will play a major role in the following as well.

As for the interaction model under study here, we are considering classical, identical particles, possessing D_{2h} symmetry, whose centers of mass are associated with a three-dimensional simple-cubic lattice. The interaction potential is isotropic in orientation space, and restricted to nearest neighbors, involving particles or sites labelled by λ and μ, respectively; the orientation of each particle can be specified via an orthonormal triplet of three-component vectors (defined by intersections of its symmetry planes, and usually coinciding with eigenvectors of its inertia or polarizability tensors), say $\{\mathbf{n}_{\lambda,j}, j = 1,2,3\}$; in turn, these are defined by an ordered triplet of Euler angles $\omega_\lambda = \{\phi_\lambda,\theta_\lambda,\psi_\lambda\}$. Orientations are defined with respect to the above common, but otherwise arbitrary, Cartesian frame. It also proves convenient to use a simpler notation for the unit vectors defining orientations of two interacting molecules [70], that is, $\mathbf{u}_j$ for $\mathbf{n}_{\lambda,j}$, and $\mathbf{v}_k$ for $\mathbf{n}_{\mu,k}$, respectively; here, for each j, $\mathbf{u}_j$ and $\mathbf{v}_j$ have the same functional dependencies on ω_λ and ω_μ, respectively (pairs of corresponding unit vectors in the two interacting molecules). Let $\tilde{\Omega} = \Omega_{\lambda\mu}$ denote the set of Euler angles defining the rotation transforming $\mathbf{u}_j$ into $\mathbf{v}_j$; Euler angles will be defined here according to the convention used by Brink and Satchler [71–73]. We also define

$$f_{jk} = (\mathbf{v}_j \cdot \mathbf{u}_k), \quad G_{jk} = P_2(f_{jk}). \tag{3}$$

The simplest continuous interaction potentials proposed and studied in this context (see, e.g., Refs. [46,47,74,75]) are quadratic with respect to the scalar products f_{jk}; owing to available geometric identities and without any loss of generality (see, e.g., the discussion in Ref. [19]), they can be reduced to a linear combination involving the three terms G_{kk} only, that is,

$$\Phi = \epsilon \sum_{k=1}^{3} r_k G_{kk}, \tag{4a}$$

or

$$\Phi = \epsilon\{\xi G_{33} + \eta(G_{11} - G_{22}) + \zeta[2(G_{11} + G_{22}) - G_{33}]\}. \tag{4b}$$

Linear transformations between the two sets of coupling constants can be found in Ref. [19]; in the present, D_{2h}-symmetric case, at most one of the three coefficients r_k can equal zero. The three coefficients in each set can be taken to be smaller than 1 in magnitude, possibly at the cost of rescaling ϵ, and hence the temperature, as will be done here (so that the available volume in parameter space is 8). Moreover, inequivalent regions of the parameter space can be further reduced, allowing for duality, that is, invariance of the pair potential upon applying the same permutation to both sets of interacting axes (see Refs. [19,46,47]). Notice also that, in Eq. (4), equality between two of the three coefficients, say $r_1 = r_2$ or equivalently the condition $\eta = 0$, entail an additional D_{4h} symmetry of the interaction [20]; in other words, two simultaneous rotations by $\pm\frac{\pi}{2}$ around the two unit vectors associated with the third coefficient, $\mathbf{u}_3$ and $\mathbf{v}_3$, respectively (i.e., taking place in the individual molecular frames), conserve the potential.

As in Refs. [20,58], we shall be considering here cases where the potential parameters, in the notation of Eq. (4a), assume the specialized values +1, 0, or −1; hence, in the corresponding names, the symbols P,0,M will be assigned accordingly; for example, the P0M model [58] is defined by $r_1 = +1, r_2 = 0, r_3 = -1$ (see other examples below).

Particle interactions, correlations, and orientational order are usually expressed in terms of symmetry-adapted combinations of Wigner rotation functions $\mathcal{D}^J_{m,n}(\omega)$, that is, for D_{2h} symmetry (see, e.g., Refs. [70,76,77], as well as detailed comparisons and discussion of notational issues in Ref. [78]):

$$R^J_{pq}(\omega) = (1/4) \sum_{s=\pm 1} \sum_{t=\pm 1} \mathcal{D}^J_{sp,tq}(\omega); \tag{5}$$

here J, p, q denote even and non-negative integers, $0 \leqslant p \leqslant J$, $0 \leqslant q \leqslant J$, and $\omega = \{\phi, \theta, \psi\}$ denotes the ordered triplet of Euler angles. Thus,

$$\begin{aligned} s_1(\omega) &= R^2_{00}(\omega) = P_2(\cos\theta), \\ s_2(\omega) &= R^2_{20}(\omega) = (1/4)\sqrt{6}\sin^2\theta\cos(2\phi), \\ s_3(\omega) &= R^2_{02}(\omega) = (1/4)\sqrt{6}\sin^2\theta\cos(2\psi), \\ s_4(\omega) &= R^2_{22}(\omega) = (1/4)(1+\cos^2\theta)[\cos(2\phi)\cos(2\psi)] \\ &\quad - (1/2)\cos\theta[\sin(2\phi)\sin(2\psi)]. \end{aligned} \tag{6}$$

In Eq. (6), the simpler symbols $s_k(\omega)$, involving just one subscript, have been defined as well, for notational convenience, especially in connection with the MF treatment of the following section. Each term G_{jk} can be expressed as a linear combination of the four above functions $R^2_{pq}(\tilde{\Omega})$ (see, e.g., Refs. [19,77]). The rather general potential model to be considered here [Eq. (4)] can also be written in terms of the above symmetry-adapted basis functions [Eq. (6)] (see also remarks on notation in Ref. [20]), that is,

$$\Phi = \epsilon \left\{ \xi s_1(\tilde{\Omega}) - \frac{\sqrt{6}}{2}\eta[s_2(\tilde{\Omega}) + s_3(\tilde{\Omega})] + 6\zeta s_4(\tilde{\Omega}) \right\}. \tag{7}$$

Over the years, various specific, biaxial mesogenic, parametrizations had been proposed and studied for Eq. (4); the first one of them, due to Straley [74] is based on an approximate mapping from a hard-parallelepiped model. Another, more often studied one [70,75,76,79,80], is $\xi = -1, 4\zeta = -\eta^2$; this can also be obtained by starting from a dispersion model at the London-de Boer-Heller approximation and isotropically averaging over the orientation of the intermolecular vector (see, e.g., Refs. [75,80]).

Both the Straley [74] and the "dispersive" parametrizations mostly predict a biaxial-to-uniaxial transition of second order, followed by a uniaxial-to-isotropic transition of first order; a direct biaxial-to-isotropic transition of second order only exists for special values of the potential parameters (isolated Landau points). As mentioned above, a new approach was started over the last few years in Refs. [46,47], along two different lines of development. On the one hand, the authors of Refs. [46,47] had examined, for general values of the parameters, the mathematical conditions under which the pair potential [Eq. (4)] produces a fully aligned biaxial pair ground state, as well as its mechanical stability; the named stability condition [46,47] reads

$$\zeta < 0, \quad \text{and} \quad |\eta| < -(\xi + \zeta), \tag{8a}$$

or

$$r_1 + r_2 < 0, \quad \text{and} \quad |r_1 - r_2| < (-1/2)(r_1 + r_2) - r_3. \tag{8b}$$

The measure of the corresponding set of points in parameter space can be more easily calculated via the notation of Eq. (8a), and is found to be 2 (i.e. one-fourth of the available volume). Notice also that the two above named sets of parameters were found to be consistent with the conditions in Eq. (8). On the other hand, the authors of [46,47] had proposed the simplified model defined by $\xi = -1, \eta = 0, \zeta < 0$, that is, $r_1 = r_2$, and studied it by MF, carrying out a bifurcation analysis of the resulting consistency equations. The existence of direct transitions between biaxial and isotropic phases, was proven, together with criteria for the existence of tricritical points. In addition to the Straley parametrization and to the "dispersive" one, models defined by other parameter values falling in the above stability region [Eq. (4)] have been studied as well [20,48,50,53,81–84]. Yet, in experimental terms, the thermotropic biaxial phase is an exception rather than the rule, and, on the other hand, the presence of three coupling constants in Eq. (4) makes the pair potential model under consideration rather versatile [i.e., capable of producing different types of orientational order in the pair ground state and hence (presumably) in low-temperature phases]. Thus, there is some interest in addressing regions of the parameter space where suitable antinematic terms prevent the existence of a biaxially ordered pair ground state; this range is defined in general by [20,46–48,50]

$$\zeta \geqslant 0, \quad \text{or} \quad |\eta| \geqslant -(\xi + \zeta), \tag{9a}$$

or

$$r_1 + r_2 \geqslant 0, \quad \text{or} \quad |r_1 - r_2| \geqslant (-1/2)(r_1 + r_2) - r_3. \tag{9b}$$

Actually, it is by now known that already the presence of one antinematic term among the three coefficients r_k *may suffice* to spoil the biaxial ground state. An example is the entropic destabilization of the fully ordered biaxial state taking place when $\xi < 0, \eta \neq 0, \zeta = 0$ in Eq. (4b) or $r_1 \neq 0, r_2 = -r_1, r_3 < 0, |r_1| \leqslant |r_3|$ in Eq. (4a); it was observed in Ref. [79], and later discussed in greater detail in Ref. [20]. On the other hand, the broader conditions $r_3 > 0, r_1 + r_3 < 0, r_2 + r_3 < 0$ may or may not satisfy Eq. (8b) (consider, e.g., the two cases $r_1 = -1, r_2 = -0.8, r_3 = +0.1$, and $r_1 = -1$, $r_2 = -0.2$, $r_3 = +0.1$).

Let us also recall that, in some cases, excluded volume between identical convex bodies (spherocuboids) have been obtained in closed form [49], and it was found that their quadrupolar projections give rise to partly repulsive interactions, still belonging to the biaxial stability region (8); on the other hand, models containing stronger antinematic contributions, such as P0M and PPM in [58], as well as PPP discussed here, might be linked with excluded volumes between hard nonconvex bodies [85].

Another class of partly antinematic potential models has been investigated in Ref. [58]. These models are defined by

$$r_1 \geqslant 0, \quad r_2 \geqslant 0, \quad r_3 < 0, \quad r_1 + r_2 > 0. \tag{10}$$

The parameter values chosen in Eq. (10) entail a nematic coupling between the long molecular axes (the $''3''$ axes $\mathbf{u}_3, \mathbf{v}_3$), and an antinematic one between other corresponding axes. The nondegenerate pair ground state can be worked out by inspection, and reads

$$\mathbf{v}_1 = \mathbf{u}_2, \quad \mathbf{v}_2 = \mathbf{u}_1, \quad \mathbf{v}_3 = \mathbf{u}_3; \tag{11}$$

owing to the bipartite character of the lattice and to the nearest-neighbor interaction, it is propagated over the whole lattice without frustration. Notice that here biaxial order is precluded on energy grounds, in contrast to the above entropic mechanism [20,79]. The two specific cases P0M ($r_1 = +1$, $r_2 = 0$, $r_3 = -1$) and PPM ($r_1 = r_2 = +1$, $r_3 = -1$) were investigated in Ref. [58]; P0M was found to produce a first-order transition between uniaxial nematic and isotropic phases. On the other hand, both PPM and its opposite MMP (Ref. [20]) showed evidence of a second-order transition.

Here we go on to investigate models from the general interaction potential (4) where the calamitic terms are completely removed and all the couplings are antinematic, that is,

$$r_1 > 0, \quad r_2 > 0, \quad r_3 > 0, \tag{12}$$

in Eq. (4a), and, more explicitly, the very simple case $r_1 = r_2 = r_3 = +1$ (PPP) in the notation of Eq. (4a), thus taking the form,

$$\Phi = \epsilon \left[G_{11} + G_{22} + G_{33} \right], \tag{13}$$

corresponding to $\xi = \frac{3}{2}$, $\eta = 0, \zeta = 1/2$ in Eqs. (4b) and (7),

$$\Phi = \epsilon \left\{ \frac{3}{2} s_1 \left(\tilde{\Omega} \right) + 3 s_4 \left(\tilde{\Omega} \right) \right\}. \tag{14}$$

Here the condition $r_1 = r_2 = r_3$ entails O_h invariance of the interaction: two simultaneous rotations by $\pm\frac{\pi}{2}$ around the two unit vectors $\mathbf{u}_i$ and $\mathbf{v}_i$ for each couple ($i = 1,2,3$), respectively (i.e., taking place in the individual molecular frames), conserve the potential. Its pair ground-state configuration is degenerate, and the combination of bipartite lattice and nearest-neighbor character of the interaction propagates it over the lattice and increases degeneracy without frustration.

The pair ground-state configuration for the PPP potential model [Eq. (13)] is doubly degenerate and can be written down by inspection; it reads

$$\begin{gathered} \mathbf{v}_1 = \mathbf{u}_2, \quad \mathbf{v}_2 = \mathbf{u}_3, \quad \mathbf{v}_3 = \mathbf{u}_1, \quad \text{or} \\ \mathbf{v}_1 = \mathbf{u}_3, \quad \mathbf{v}_2 = \mathbf{u}_1, \quad \mathbf{v}_3 = \mathbf{u}_2; \end{gathered} \tag{15}$$

other critical points can be worked out and invariably lead to a higher energy. For each of the above pair configurations, the Hessian matrix was found to be positive definite.

Actually, since we are interested in overall ground-state configurations as well, it proves convenient to describe them in a more general setting (i.e., by expressing particle orientations in the common Cartesian frame); let thus single-particle orientations E_1, E_2, E_3 be defined as follows:

$$\mathbf{n}_{\lambda,1} = \mathbf{e}_1, \mathbf{n}_{\lambda,2} = \mathbf{e}_2, \mathbf{n}_{\lambda,3} = \mathbf{e}_3, \quad \text{for } E_1; \tag{16a}$$

$$\mathbf{n}_{\lambda,1} = \mathbf{e}_2, \mathbf{n}_{\lambda,2} = \mathbf{e}_3, \mathbf{n}_{\lambda,3} = \mathbf{e}_1, \quad \text{for } E_2; \tag{16b}$$

$$\mathbf{n}_{\lambda,1} = \mathbf{e}_3, \mathbf{n}_{\lambda,2} = \mathbf{e}_1, \mathbf{n}_{\lambda,3} = \mathbf{e}_2, \quad \text{for } E_3. \tag{16c}$$

At this stage, one recognizes that the set of configurations DA (and hence its subsets DB and DC) can be defined for PPP by the appropriate transcription of the above stipulations for KS: In other words, orientation of particle $\mathbf{s}_\lambda$ along a certain $\pm\mathbf{e}_k$ for the KS model corresponds to orientation of the triplet $\{\mathbf{n}_{\lambda,j}\}$ along E_k for the PPP model. Comparison with KS shows an important difference: Since the continuous degeneracy (hence the CC set of configurations) has disappeared here, DA now exhausts all ground-state configurations. Notice also that the ground state of PPP possesses no second-rank orientational order, but a fourth-rank cubatic one, by the above O_h symmetry of the interaction.

Calculation of the orientational order parameters for a configuration of type DC yields

$$\begin{gathered} \langle s_1' \rangle_{DC} = 1, \quad \langle s_4' \rangle_{DC} = (1/2), \quad \langle s_2' \rangle_{DC} = \langle s_3' \rangle_{DC} = 0, \\ \langle s_1'' \rangle_{DC} = -(1/2), \quad \langle s_4'' \rangle_{DC} = -(1/4), \\ \langle s_2'' \rangle_{DC} = \langle s_3'' \rangle_{DC} = 0; \end{gathered}$$

here prime and double prime label quantities associated with the two named even and odd sublattices, and overall quantities are given by the corresponding arithmetic averages, that is,

$$\langle s_1 \rangle_{DC} = (1/4), \quad \langle s_4 \rangle_{DC} = (1/8), \quad \langle s_2 \rangle_{DC} = \langle s_3 \rangle_{DC} = 0,$$

and

$$\langle P_4 \rangle_{DC} = 11/16.$$

At this stage, it is appropriate to recall the definition of q-state Potts models [86]: Let q denote a positive integer, $q > 1$, and for each lattice site let there be associated a variable $\kappa_\lambda \in \{1,2,\ldots,q\}$; interactions (restricted to nearest neighbors in the simplest cases) are defined by

$$\Psi = \mp\epsilon \delta_{\kappa_\lambda, \kappa_\mu}, \tag{17}$$

where the sign defines the ferro—or antiferro—magnetic character of the interaction.

A similar line of reasoning as above now shows that the set DA of ground-state configurations for PPP can be reinterpreted as the set of ground-state configurations for the antiferromagnetic three-state Potts model [86] (in other words, the triplet $\{\mathbf{n}_{\lambda,j}\}$ in orientation E_k for the PPP model corresponds to the local Potts variable κ_λ having the value k). At finite temperatures, the difference between continuous site variables for PPP and discrete ones for the corresponding three-state Potts models will set in; on the other hand, one can at least think of a low-temperature régime where the above mapping may still offer some guidance.

Actually, the three-state antiferromagnetic Potts model on a simple-cubic lattice has been rather extensively studied (see, e.g., Refs. [87–90] and others quoted therein); a recent estimate for its ground-state entropy (in units k_B per particle) is $S(0) = 0.3670 \pm 0.0001$ [90]. Moreover, simulation results yield evidence of a low-temperature broken-symmetry phase, where configurations of the DB type remain dominant; at higher temperature, the model predicts a second-order transition to the orientationally disordered phase, and a recent estimate of the transition temperature is $\Theta_{\text{Potts,MC}} = 1.222 \pm 0.004$ [90]. This result can be translated back to our PPP context, suggesting the possible existence of a low-temperature phase possessing overall biaxial order (i.e., where thermal fluctuations select

configurations of the DC type or close to it), as will be shown in the following.

III. MOLECULAR FIELD ASPECTS

It seems appropriate to start this section with a couple of remarks, addressing comparison and contrast with other relevant references, especially Ref. [51].

On the one hand, in keeping with the MC framework and with usual MF calculations for bulk systems, we are considering a periodically repeated cubic sample, consisting of N sites, where N is the cube of an even number, and involving 3N distinct nearest-neighboring interacting pairs. The coordination parameter z defined in [51], Eq. (4.12), would accordingly correspond to the value $\rho = 6$ used here; notice however that the value quoted in Ref. [51] (Table 1, page 155) does not allow for periodicity, and that the difference becomes negligible in the thermodynamic limit.

On the other hand, some different comparisons with Ref. [51] are in order as well; as pointed out above, Eq. (8) defines a region in the parameter space for the gS model [Eq. (4)] producing a stable biaxial pair ground state. The corresponding MF treatment (possibly using a general minimax strategy [48,51]) is based on a single set of variational parameters. In other words, the MF treatment can be adapted to and tested on a lattice model, which is also studied by simulation, and the MF order parameters are to be interpreted as describing uniform biaxial order; however, this does not exhaust the potentialities of the gS model. Actually, the choices P0M and PPM in Ref. [58] produce a different pair ground state, and hence a different overall (staggered) ground state, for which the uniform-lattice MF approach turned out to be inadequate, especially for PPM, basically because it does not even reproduce the pair ground state; similarly, for the KS model, a uniform-lattice MF treatment was proven to yield only orientational disorder at all positive temperatures [50]. Such an approach was also attempted here for PPP, and numerically found to yield only the isotropic (orientationally disordered) phase as the stable one at all positive temperatures.

Notice also that an MF treatment properly allowing for the above DC-type configurations would require a cubic sample consisting of 2^3 particles in three different orientations; therefore, following also the line of thought of our previous paper [58], we have chosen the approach outlined below, based on a further simplification of a two-sublattice procedure from Refs. [58,62] (i.e., the simplest treatment qualitatively consistent with available ground-state information, cubatic symmetry of the interaction, and overall results of MC simulation).

Thus, following the named two-sublattice framework [58,62], we shall be using two sets of symmetry-adapted basis functions $s'_j = s'_j(\omega)$, $s''_k = s''_k(\omega)$, one for each (even or odd) sublattice, where j and k range between 1 and 4, $s'_j(\omega)$ has the same functional dependence on ω as $s''_j(\omega)$ [see Eqs. (5) and (6)], and the superscript accounts for the sublattice. The symbols $\langle s'_j\rangle$ and $\langle s''_k\rangle$ will similarly represent the corresponding sublattice order parameters; overall lattice order parameters will in turn be computed as arithmetic mean of the corresponding pair of sublattice quantities, $\langle s_k\rangle = (1/2)(\langle s'_k\rangle + \langle s''_k\rangle)$. In the framework of Refs. [58,62], $\langle s'_j\rangle$ and $\langle s''_k\rangle$ correspond to each sublattice being homogeneously ordered, whereas, in the simplified treatment implemented here, some of them are rather to be interpreted as effective averages over a sublattice (recall DC configurations in the previous section); notice also that s'_j and s''_k correspond to p_j and q_k in Ref. [58].

In the named two-sublattice treatment, the free energy in units ϵ per site would read

$$A^*_{\mathrm{MF}} = \sigma \sum_{j=1}^{4}\sum_{k=1}^{4} d_{jk}\langle s'_j\rangle\langle s''_k\rangle - \frac{T^*}{2}\left[\ln\left(\frac{Z_1}{8\pi^2}\right) + \ln\left(\frac{Z_2}{8\pi^2}\right)\right], \tag{18}$$

$$W_2 = \sum_{j=1}^{4}\sum_{m=1}^{4} d_{jm}\langle s''_j\rangle s'_m(\omega_1), \quad E_2 = \exp(\rho\beta W_2), \tag{19}$$

$$Z_2 = \int_{Eul1} E_2 d\omega_1, \tag{20}$$

$$W_1 = \sum_{j=1}^{4}\sum_{m=1}^{4} d_{jm}\langle s'_j\rangle s''_m(\omega_2), \quad E_1 = \exp(\rho\beta W_1), \tag{21}$$

$$Z_1 = \int_{Eul2} E_1 d\omega_2; \tag{22}$$

here $\beta = \frac{1}{T^*}$, $T^* > 0$, $\sigma = \rho/2 = 3$, where ρ denotes the lattice coordination number, and the symmetric coupling matrix $\mathbf{d}$, with entries d_{jk}, is defined by

$$[\mathbf{d}] = \begin{bmatrix} -\xi & 0 & +\frac{\sqrt{6}}{2}\eta & 0 \\ 0 & -2\xi & 0 & +\sqrt{6}\eta \\ +\frac{\sqrt{6}}{2}\eta & 0 & -6\zeta & 0 \\ 0 & +\sqrt{6}\eta & 0 & -12\zeta \end{bmatrix}. \tag{23}$$

The corresponding resulting consistency equations are

$$\langle s'_j\rangle = \frac{\int_{Eul1} s'_j(\omega_1) E_2 d\omega_1}{Z_2}, \quad j = 1,2,3,4; \tag{24}$$

$$\langle s''_k\rangle = \frac{\int_{Eul2} s''_k(\omega_2) E_1 d\omega_2}{Z_1}, \quad k = 1,2,3,4. \tag{25}$$

After solving the above consistency equations, the stable phases would eventually be identified with the solutions corresponding to the least free energy. Such a stability criterion is further elaborated in Appendix A for the very simplified case to be discussed here: The local stability criterion provided there is closely related to the one employed in the above-mentioned minimax treatment.

Actually, bearing also in mind the approach followed in Ref. [58], the above outlined general procedure can be further simplified from the start, taking into account other information available for the problem at hand, that is, by requesting

$$\begin{gathered} \langle s'_2\rangle = \langle s'_3\rangle = 0, \quad \langle s''_2\rangle = \langle s''_3\rangle = 0, \\ \langle s'_1\rangle = 2\langle s'_4\rangle, \quad \langle s''_1\rangle = 2\langle s''_4\rangle, \end{gathered} \tag{26}$$

and thus reducing to a numerically more tractable two-parameter problem, where $\langle s'_4\rangle$ and $\langle s''_4\rangle$ are expected to have opposite signs (see Appendix A for details). Such a reduction is a consequence of the O_h invariance of the pair potential (see Refs. [50,53]), entailing the possible ordered phase to be biaxial.

Accordingly, we get the effective free energy,

$$A^*_{\rm MF} = -36\langle s'_4\rangle\langle s''_4\rangle - \frac{T^*}{2}\left[\ln\left(\frac{Z_1}{8\pi^2}\right) + \ln\left(\frac{Z_2}{8\pi^2}\right)\right], \tag{27}$$

with the sublattice partition functions,

$$\begin{aligned} Z_2 &= \int_{Eul1} \exp[-18\beta\langle s''_4\rangle s'_5(\omega_1)]d\omega_1, \\ Z_1 &= \int_{Eul2} \exp[-18\beta\langle s'_4\rangle s''_5(\omega_2)]d\omega_2, \end{aligned} \tag{28}$$

where the symbols,

$$\begin{aligned} s'_5 &= s'_5(\omega) = s'_1(\omega) + 2s'_4(\omega), \\ s''_5 &= s''_5(\omega) = s''_1(\omega) + 2s''_4(\omega) \end{aligned} \tag{29}$$

have been introduced for notational convenience. Notice also that $A^*_{\rm MF}$ is invariant under the interchange between $\langle s'_4\rangle$ and $\langle s''_4\rangle$, corresponding to the interchange of the two sublattices.

Thus the MF consistency equations read

$$\frac{\partial A^*_{\rm MF}}{\partial\langle s''_4\rangle} = -36\langle s'_4\rangle + 9\frac{\int_{Eul1} s'_5(\omega_1)\exp[-18\beta\langle s''_4\rangle s'_5(\omega_1)]d\omega_1}{Z_2} = 0, \tag{30}$$

$$\frac{\partial A^*_{\rm MF}}{\partial\langle s'_4\rangle} = -36\langle s''_4\rangle + 9\frac{\int_{Eul2} s''_5(\omega_2)\exp[-18\beta\langle s'_4\rangle s''_5(\omega_2)]d\omega_2}{Z_1} = 0. \tag{31}$$

By the above O_h symmetry [Eq. (26)], Eqs. (30) and (31) are equivalent to

$$\langle s'_4\rangle = \frac{\int_{Eul1} s'_4(\omega_1)\exp[-18\beta\langle s''_4\rangle s'_5(\omega_1)]d\omega_1}{Z_2}, \tag{32}$$

$$\langle s''_4\rangle = \frac{\int_{Eul2} s''_4(\omega_2)\exp[-18\beta\langle s'_4\rangle s''_5(\omega_2)]d\omega_2}{Z_1}, \tag{33}$$

that is, they correspond to the appropriate specializations of Eqs. (24) and (25). A bifurcation analysis of the above equations has been carried out [91] and a bifurcation temperature has been found at $\beta = 5/9$ ($\Theta_{\rm PPP,MF} = 9/5$), where a second-order transition takes place from the isotropic phase. The bifurcation equations also show that the bifurcating order parameter branches are such that $\langle s'_4\rangle = -\langle s''_4\rangle$ at their onset (see also Appendix A for details), with

$$\langle s'_4\rangle = \frac{147}{275}\sqrt{\frac{5}{33\,\Theta_{\rm PPP,MF}}}\sqrt{\Theta_{\rm PPP,MF} - T^*} + O((\Theta_{\rm PPP,MF} - T^*)). \tag{34}$$

Accordingly, calculation of the free energy along these branches (i.e., of the least-free-energy values) delivers

$$A^*_{\rm MF} = -\frac{147}{55\,\Theta^2_{\rm PPP,MF}}(\Theta_{\rm PPP,MF} - T^*)^2 + O((\Theta_{\rm PPP,MF} - T^*)^3). \tag{35}$$

The consistency equations were also solved numerically starting at a much lower temperature and for increasing values of it, and the above result was confirmed; in the low-temperature regime the two-order parameters were found to saturate to $\frac{1}{2}$ and $-\frac{1}{4}$, respectively, thus giving for the overall order parameters,

$$\langle s_1\rangle = 2\langle s_4\rangle = \tfrac{1}{4}, \tag{36}$$

in agreement with MC simulation results and with results for the above DC ground-state configurations. The MF expression for the potential energy becomes in this case [58],

$$U^*_{\rm MF} = 36\langle s'_4\rangle\langle s''_4\rangle, \tag{37}$$

from which the configurational specific heat was calculated by numerical differentiation.

Let us recall that both MF and TSC treatments have been worked out for the KS model; their estimates for the transition temperatures are $\Theta_{\rm KS,MF} = 6/5$ and $\Theta_{\rm KS,TSC} = 4/5$, respectively [62], and the latest simulation estimate for the transition temperature is $\Theta_{\rm KS,MC} = 0.6227 \pm 0.0001$ [63].

IV. SIMULATION ASPECTS

The simulation methodology used here closely followed our previous papers on the subject [20,52,58]. We used a periodically repeated cubic sample, consisting of $N = l^3$ particles, $l = 10,20,30$, and ran calculations in cascade, in order of increasing temperature; each cycle (or sweep) consisted of $2N$ MC steps, including a sublattice sweep [92]. Equilibration runs took between 25 000 and 200 000 cycles, and production runs took between 250 000 and 1 250 000; macrostep averages for evaluating statistical errors were taken over 1000 cycles. Calculated thermodynamic quantities include mean potential energy U^* (in units ϵ per site) and configurational specific heat per particle C_V. Simulation estimates of the overall second-rank order parameters $\langle R^2_{pq}\rangle = \langle s_k\rangle, k = 1,2,3,4$ [64,66,78,93] were calculated by analyzing a configuration every cycle, using methodologies discussed in detail by other authors [66,76,94,95]; the nematic fourth-rank order parameter $\langle P_4\rangle$ was calculated as well ([60,64–66]).

Notice also that, by the underlying O_h symmetry, one expects for PPP that $\langle s_2\rangle = \langle s_3\rangle = 0$, and $\langle s_1\rangle = 2\langle s_4\rangle$, as discussed in detail elsewhere [50,53] and as recalled in Sec. III. The so-called short-range order parameters were evaluated as well, defined by [64,66]

$$\sigma_{L,j} = \langle P_L(f_{jj})\rangle, \quad L = 2,4, \quad j = 1,2,3, \tag{38}$$

and measuring correlations between corresponding pairs of unit vectors associated with nearest-neighbor molecules. Equation (4) implies that the potential energy U^* is a linear combination of the quantities $\sigma_{2,j}$. Actually, in the present case, the underlying O_h symmetry entails $\sigma_{L,1} = \sigma_{L,2} = \sigma_{L,3}$, and this common value will be denoted by $\sigma_{L,c}$; the potential energy is proportional to the appropriate common value (i.e., $U^* = +9\sigma_{2,c}$). The above Eq. (37) can be used to define the MF estimate $\sigma_{2,c,\rm MF} = 4\langle s'_4\rangle\langle s''_4\rangle$. In the calculations, at the end of each macrostep, we carried out a rotation of each particle by $\frac{\pi}{2}$ around its $\mathbf{u}_3$ axis [20]; simulation results obtained in

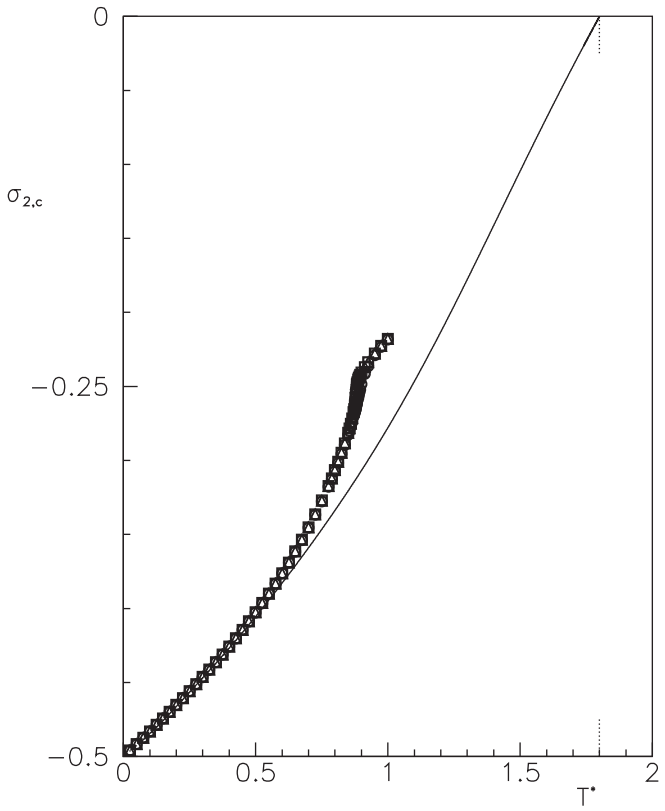

FIG. 1. MF predictions (continuous curve) and simulation results (discrete symbols) for the short-range order parameter $\sigma_{2,c}$, obtained with different sample size. The meaning of symbols is as follows: circles, $l = 10$; squares, $l = 20$; triangles, $l = 30$. Unless explicitly stated or shown, here and in the following figures, the associated statistical errors fall within the relative symbol sizes.

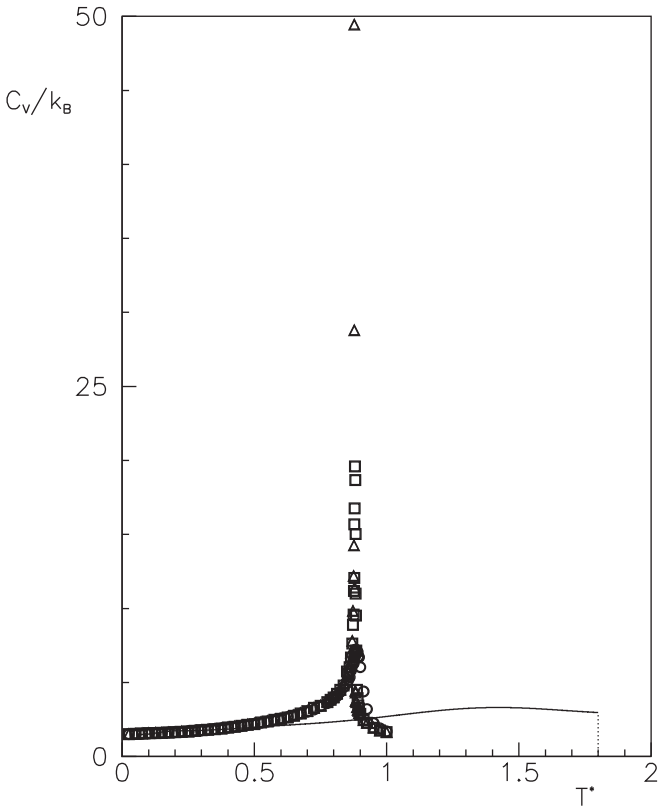

FIG. 2. MF predictions (continuous curve) and simulation results (discrete symbols) for the configurational specific heat, obtained with different sample size. Same meaning of symbols as in Fig. 1; the associated statistical errors, not shown, range between 1% and 5%.

this way for $\sigma_{L,j}$ were found to satisfy the above symmetry condition within associated statistical errors.

We also calculated the cubatic order parameter τ_4, as well as its associated susceptibility χ_4, defined as follows [17,96]. Let

$$M_4 = \sqrt{\left(\frac{4}{21}\right)\sum_{\lambda=1}^{N}\sum_{\mu=1}^{N}\left[\sum_{j=1}^{3}\sum_{k=1}^{3}P_4(\mathbf{n}_{\lambda,j}\cdot\mathbf{n}_{\mu,k})\right]}; \quad (39)$$

then the simulation estimate for the cubatic order parameter is

$$\tau_4 = \frac{1}{N}\langle M_4\rangle, \quad (40)$$

and its associated susceptibility reads

$$\chi_4 = \frac{1}{N}\beta\left(\langle M_4^2\rangle - \langle M_4\rangle^2\right). \quad (41)$$

Computational aspects of Eq. (39) are discussed in Refs. [17,96]. The cubatic counterpart of Eq. (38), defined by [17,96]

$$\sigma_{4,4} = \frac{4}{21}\left\langle\sum_{j=1}^{3}\sum_{k=1}^{3}P_4(f_{jk})\right\rangle, \quad (42)$$

was calculated as well.

The simulation results reported in the following were obtained starting at low temperature from a ground-state configuration of the above DC type; as a check, additional simulations were carried out for $l = 10$ and starting from a D3 configuration. The obtained results exhibited a far weaker orientational order, and, at $T^* \approx 0.7$, they appeared to jump irreversibly to the above DC branch: The change involved a mild but recognizable decrease in $\sigma_{2,c}$ (hence the potential energy), from -0.33 to -0.34 and a pronounced increase in orientational order, with $\langle s_1\rangle$ changing from 0.02 to 0.14; moreover, upon decreasing the temperature, the obtained simulation results continued to follow the DC branch.

V. RESULTS AND COMPARISONS

Simulation results, and available MF predictions, are plotted in the following Figs. 1–8.

Results for $\sigma_{2,c}$ (i.e., essentially the potential energy), reported in Fig. 1, were found to be hardly dependent on sample size: Actually, in the temperature range between $T^* = 0.85$ and $T^* = 0.95$, sample-size dependency appeared to saturate for $l \geqslant 20$; outside this range, simulation results for the three named sizes were found to coincide to within symbol sizes. Moreover, the results were found to evolve with temperature in a gradual and continuous way, and suggested a change of slope taking place around $T^* \approx 0.875$.

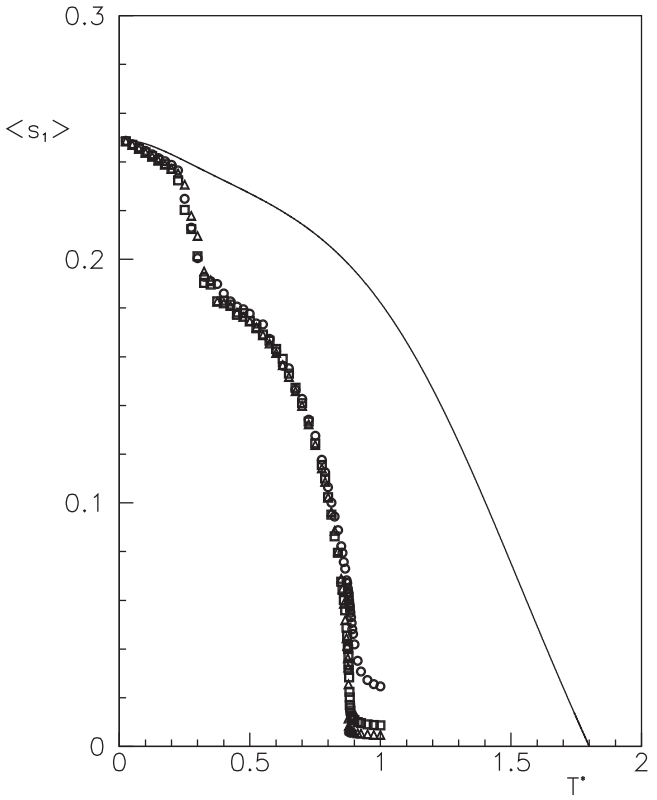

FIG. 3. MF predictions (continuous curve) and simulation results (discrete symbols) for the long-range order parameter $\langle P_2 \rangle = \langle s_1 \rangle$, obtained with different sample sizes; same meaning of symbols as in Fig. 1.

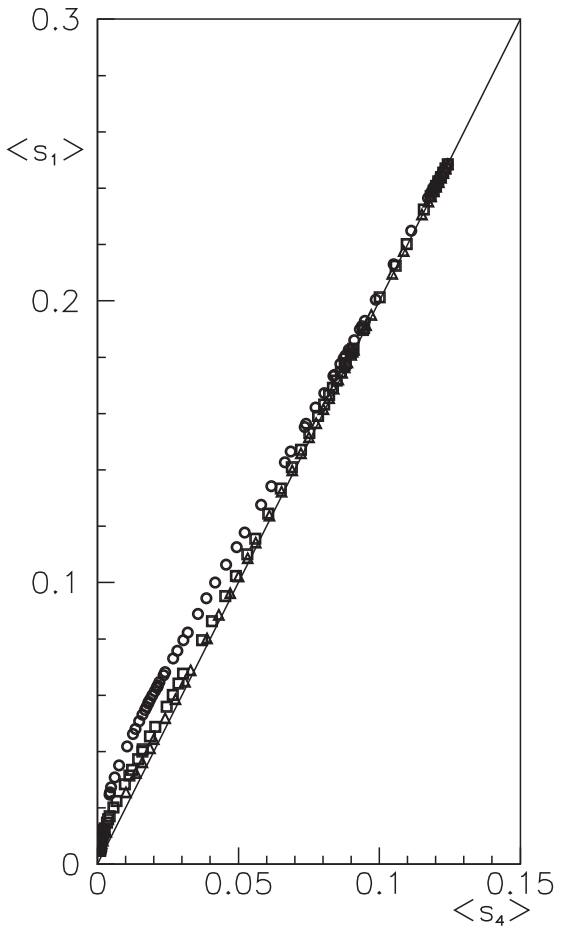

FIG. 4. Plots of simulation results for the long-range order parameter $\langle s_1 \rangle$, obtained with different sample sizes, versus the corresponding results for $\langle s_4 \rangle$, for the same sample sizes; same meaning of symbols as in Fig. 1; the continuous segment corresponds to the O_h symmetry relation $\langle s_1 \rangle = 2\langle s_4 \rangle$.

Simulation results for the configurational specific heat (Fig. 2) were also found to be independent of sample size for $T^* \leqslant 0.85$ and then again for $T^* \geqslant 0.95$, and exhibited a recognizable sample-size dependency in between, where the height of the peak at $T^* \approx 0.875$ appeared to increase with increasing sample size.

On the whole, Figs. 1 and 2 show a good agreement between MF predictions and simulation results in a low-temperature range, say $T^* \lesssim 0.4$ at least.

Simulation results for $\langle P_2 \rangle = \langle s_1 \rangle$ (Fig. 3) exhibited a gradual and monotonic decrease with temperature, and a recognizable decrease with increasing sample size for $T^* \gtrsim 0.85$. Simulation results for $\langle P_2 \rangle = \langle s_1 \rangle$ are plotted versus their counterparts for $\langle R_{22}^2 \rangle = \langle s_4 \rangle$ in Fig. 4; the graph was consistent with the O_h symmetry relation $\langle s_1 \rangle = 2\langle s_4 \rangle$ [50,53], and the agreement was found to improve with increasing sample size. Notice also in Fig. 3 that the plot of simulation results, but not of the MF prediction, seems to show an inflection point at low temperature, possibly pointing to an effect of thermal fluctuations which MF cannot reproduce well. Simulation results for the orientational order parameters $\langle R_{20}^2 \rangle = \langle s_2 \rangle$ and $\langle R_{02}^2 \rangle = \langle s_3 \rangle$ (figures not shown) were found to be smaller than ≈ 0.006; their temperature evolution showed a peak around $T^* \approx 0.875$. Moreover, at all investigated temperatures, they exhibited a pronounced decrease with increasing sample size, suggesting their vanishing in the thermodynamic limit.

Structural quantities measuring short-range correlations of rank 4 (i.e., $\sigma_{4,c}$ and $\sigma_{4,4}$), respectively, exhibited a monotonic and gradual decay with temperature, a change of slope around $T^* \approx 0.875$, and no recognizable sample-size dependency. Simulation results obtained for both observables with the largest investigated sample size $l = 30$, are plotted together and compared in Fig. 5.

The long-range order parameter $\langle P_4 \rangle$ (Fig. 6) exhibited a continuous decay with temperature, and sample-size dependency only becoming recognizable at $T^* \gtrsim 0.85$; the cubatic order parameter τ_4 (Fig. 7) also exhibited a continuous decay with temperature, and showed a sample-size dependency saturating for $l \geqslant 20$. Notice also that MC and MF plots for $\langle P_4 \rangle$ suggest different curvatures.

The cubatic susceptibility χ_4 (Fig. 8) showed a pronounced sample-size dependency as well as a peak at a temperature corresponding to the abscissa of the peak of the configurational specific heat, growing higher with increasing sample size.

Notice also that plots for various simulated quantities exhibit a linear evolution with temperature in some low-temperature range, up to $T^* = 0.25$ at least; this trend is especially pronounced for fourth-rank short-range order

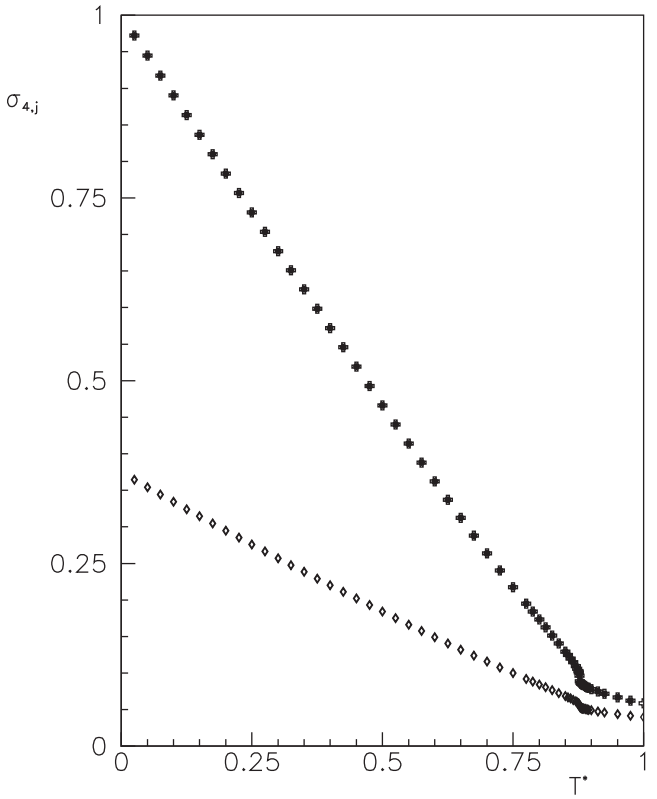

FIG. 5. Simulation results for the cubatic short-range order parameters $\sigma_{4,c}$ (diamonds) and $\sigma_{4,4}$ (crosses), obtained with the largest investigated sample size $l = 30$.

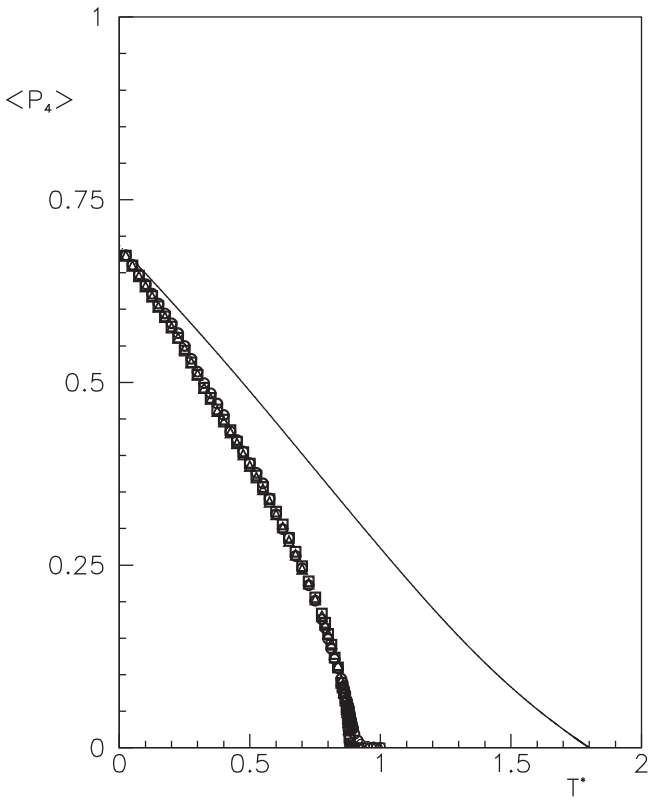

FIG. 6. MF predictions (continuous curve) and simulation results (discrete symbols) for the long-range order parameters $\langle P_4 \rangle$, obtained with different sample sizes; same meaning of symbols as in Fig. 1.

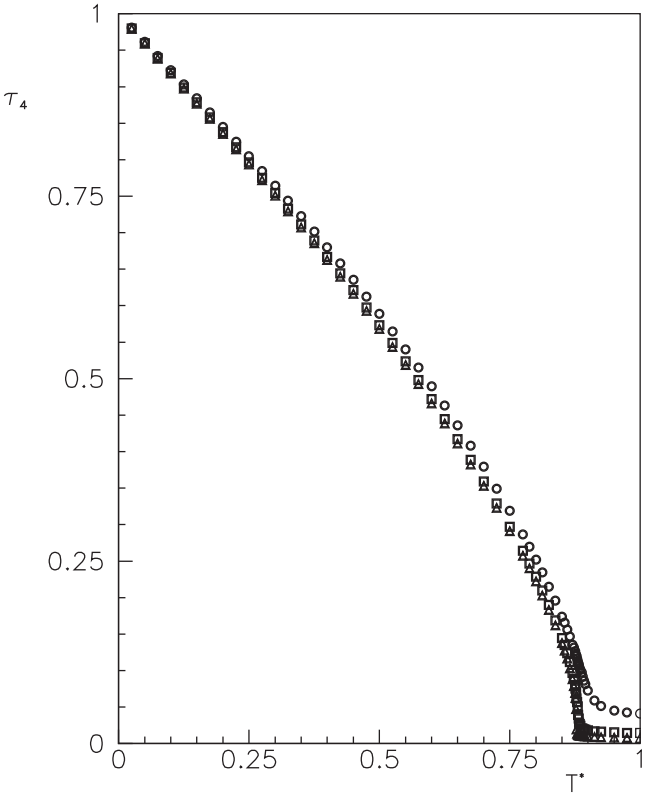

FIG. 7. Simulation results for the long-range cubatic order parameters τ_4, obtained with different sample sizes; same meaning of symbols as in Fig. 1.

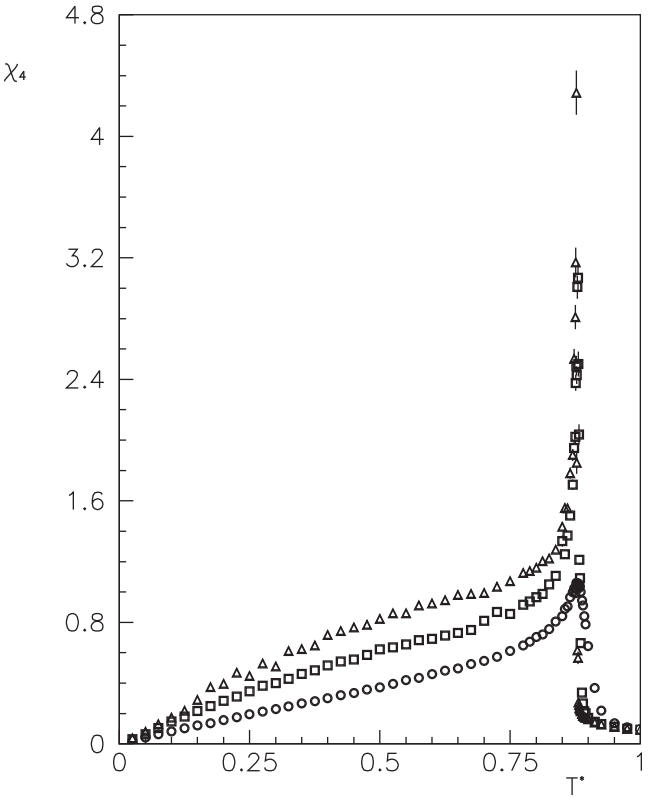

FIG. 8. Simulation results for the cubatic susceptibilty χ_4, obtained with different sample sizes; same meaning of symbols as in Fig. 1.

parameters (σ_4 in Fig. 5), but is also recognizable for their long-range counterparts (Figs. 6 and 7). On the other hand, Figs. 6, 7, and 12 in Ref. [58] also show a similar behavior for some $\sigma_{L,j}$ of models P0M and PPM; on the whole, comparisons suggest that this behavior is more pronounced for pairs interacting via a positive (repulsive) coupling constant.

To summarize, the present simulation results suggest a second-order transition; the transition temperature is conservatively estimated to be $\Theta_{\mathrm{PPP,MC}} = 0.88 \pm 0.01$.

Comparison between MF and MC, as well as with the corresponding results obtained for KS [61–63] (see also previous section), shows that the simplified MF treatment used here still yields a reasonable qualitative picture, but overestimates the transition temperature by a factor 2.

VI. CONCLUSIONS

As already pointed out, the gS potential model in Eq. (4) is rather versatile, and the presence in it of sizable antinematic terms may entail important effects of the lattice geometry [58], as well as the need of a more refined (but still simplified) MF approach.

We have studied here an extreme, fully antinematic case, where the three coupling constants are set to a common positive value; its pair ground state is doubly degenerate, and the combination of bipartite lattice and nearest-neighbor interaction propagates it over the lattice, increasing the overall degeneracy but without producing frustration. As explained above, one can establish meaningful connections and comparisons with both KS and the three-state antiferromagnetic Potts model (on the same simple-cubic lattice).

In the KS case, a continuously degenerate ground state also possesses overall uniaxial second-rank order. Both the present PPP and the three-state antiferromagnetic Potts model essentially involve discrete ground-state degeneracies, and an appropriate type of orientational order appears at sufficiently low but finite temperature, because the corresponding ground-state configurations are selected by thermal fluctuations (order via disorder; [67–69]). At higher temperatures, the three models appear to support a continuous transition to an orientationally disordered phase. MF treatments had been worked out for both KS and the present PPP model; they were found to produce a second-order transition and a broad qualitative agreement with simulation results, and to overestimate the transition temperature by a factor 2.

It may be appropriate to recall similarities and differences between models MMP [20], P0M, PPM [58], and the present PPP: The presence of one suitable antinematic coupling destroys biaxiality (already in the pair ground state) via an entropic mechanism, and a second antinematic term disfavors biaxiality in energetic terms (and similarly for P0M). The third antinematic coupling produces the subtle and probably unexpected effects discussed here, that is, destruction of the pair biaxial ground state, but restoration of overall biaxial order through an entropic effect, at low but finite temperature. Notice also that, in the named cases, the presence of two equal coupling constants in Eq. (4), and of a third one with the same magnitude, appear to be linked with the second-order character of the transition. Estimates for the transition temperatures for the named models are

$\Theta_{\mathrm{MMP,MF}} = 9/5$, $\Theta_{\mathrm{MMP,MC}} = 1.075 \pm 0.005$ for MMP [20];
$\Theta_{\mathrm{P0M,MF1}} = 1.0899$, $\Theta_{\mathrm{P0M,MF2}} = 1.1933$, $\Theta_{\mathrm{P0M,MC}} = 1.018 \pm 0.001$ for P0M [58];

$\Theta_{\mathrm{PPM,MF2}} = 9/5$, $\Theta_{\mathrm{PPM,MC}} = 1.455 \pm 0.005$ for PPM [58].

(In Ref. [58], MF1 and MF2 label the uniform-lattice and two-sublattice MF treatments, respectively.)

Comparisons between these numbers point to the rather well-known fact that an MF treatment yields a better agreement with simulation for first-order than for second-order transitions.

One can also envisage other similar models, involving predominantly antinematic couplings, and where the above uncoupling condition is removed, so that frustration sets in; this can be realized by extending the interactions to more distant neighbors, or by different lattice types (e.g., FCC or diamond lattice). Alternatively, one can define interaction models where particle center-of-mass coordinates sweep $\mathbb{R}^3$ and the orientational interaction has the above angular form, modulated by some function of the distance between centers of mass. To the best of our knowledge, not even their counterparts involving $D_{\infty h}$-symmetric particles have been addressed.

On the other hand, another extreme case of Eq. (4) can be envisaged, obtained by setting one coupling constant to zero and the other two to a common positive value in Eq. (4a) (PP0 model), thus producing a trebly degenerate pair ground state [Eqs. (11) and (15)]; a preliminary study suggests overall uniaxial antinematic order at low temperature. Actually, PP0 can be regarded as a limiting case of models defined by $r_1 = r_2 = +1$, $-1 < r_3 < 0$; according to available MF calculations [58], they support a second-order uniaxial-to-isotropic transition at low temperature. On the other hand, preliminary simulations also suggest the possibility of antinematic order at low but finite temperature, when r_3 becomes sufficiently small in magnitude. Work along these lines is in progress and will be reported in due course.

ACKNOWLEDGMENTS

The present extensive calculations were carried out on, among other machines, workstations belonging to the Sezione di Pavia of Istituto Nazionale di Fisica Nucleare (INFN). Allocations of computer time by the Computer Centre of Pavia University and Consorzio Interuniversitario Lombardo per l' Elaborazione Automatica (CILEA), Segrate, Milan, as well as by Centro Interuniversitario Nord-Est di Calcolo Automatico (CINECA), Casalecchio di Reno, Bologna, and Centro Interuniversitario per le Applicazioni di Supercalcolo per Università e Ricerca (CASPUR), Rome are gratefully acknowledged. The authors also thank Professor E. G. Virga (Pavia, Italy) for helpful discussion and suggestions.

APPENDIX: MOLECULAR FIELD: MATHEMATICAL ASPECTS

Here we present mathematical details about stability assessment for ordered phases in the MF approximation (see

Sec. III), essentially following the same line of reasoning as in [51].

Let us start from the effective free energy (27), depending on the two variables $\langle s_4' \rangle, \langle s_4'' \rangle$ and the temperature parameter T^*, and rewrite it for notational convenience as follows:

$$E(\langle s_4' \rangle, \langle s_4'' \rangle; T^*) = A^*_{\mathrm{MF}} = -\frac{T^*}{2} \ln \left[\frac{1}{(8\pi^2)^2} \int_{Eul1} \int_{Eul2} \times \exp\{-18\beta[\langle s_4' \rangle s_5''(\omega_2) + \langle s_4'' \rangle s_5'(\omega_1) - 4\langle s_4'' \rangle \langle s_4' \rangle]\} d\omega_2 d\omega_1 \right]. \quad \text{(A1)}$$

The above consistency equations can also be conveniently rewritten:

$$\langle s_4' \rangle = \Xi(\langle s_4'' \rangle; T^*), \quad \langle s_4'' \rangle = \Xi(\langle s_4' \rangle; T^*), \quad \text{(A2)}$$

where

$$\Xi(x; T^*) := \frac{1}{4} \frac{\int_{\mathrm{Eul}} s_5(\omega) \exp[-18\beta x s_5(\omega)] d\omega}{\int_{\mathrm{Eul}} \exp[-18\beta x s_5(\omega)] d\omega} = \frac{\int_{\mathrm{Eul}} s_4(\omega) \exp[-18\beta x s_5(\omega)] d\omega}{\int_{\mathrm{Eul}} \exp[-18\beta x s_5(\omega)] d\omega}. \quad \text{(A3)}$$

This notation shows even more clearly that each sublattice order parameter depends explicitly on the other one, and that the functional dependence is the same in both cases (sublattice flipping symmetry).

Straightforward calculations lead to the following general expressions for the second derivatives of E (which hold at any point, whether stationary or not):

$$\frac{\partial^2 E}{\partial \langle s_4' \rangle^2} = -162\beta \left\{ \frac{1}{Z_1} \int_{Eul2} [s_5''(\omega_2) - \langle s_5'' \rangle]^2 \times \exp[-18\beta \langle s_4' \rangle s_5''(\omega_2)] d\omega_2 \right\} < 0, \quad \text{(A4a)}$$

$$\frac{\partial^2 E}{\partial \langle s_4'' \rangle^2} = -162\beta \left\{ \frac{1}{Z_2} \int_{Eul1} [s_5'(\omega_1) - \langle s_5' \rangle]^2 \times \exp[-18\beta \langle s_4'' \rangle s_5'(\omega_1)] d\omega_1 \right\} < 0, \quad \text{(A4b)}$$

$$\frac{\partial^2 E}{\partial \langle s_4' \rangle \partial \langle s_4'' \rangle} = -36. \quad \text{(A4c)}$$

The negative sign of both pure second derivatives (A4a) and (A4b) is a consequence of the total repulsion (antinematicity) of the pair potential.

At this stage we can define the *deflated* free energy by

$$H(\langle s_4' \rangle; T^*) = E(\langle s_4' \rangle, \Xi(\langle s_4' \rangle; T^*); T^*) = -\frac{T^*}{2} \ln \left[\frac{1}{(8\pi^2)^2} \int_{Eul1} \int_{Eul2} \times \exp\{-18\beta[\langle s_4' \rangle s_5''(\omega_2) + \Xi(\langle s_4' \rangle; T^*) \times s_5'(\omega_1) - 4\Xi(\langle s_4' \rangle; T^*) \langle s_4' \rangle]\} d\omega_2 d\omega_1 \right]. \quad \text{(A5)}$$

It turns out that the stationary points of E [i.e., the solutions of the consistency Eqs. (30) and (31)] are in one-to-one correspondence with the stationary points of H with respect to $\langle s_4' \rangle$.

Moreover, the stable phases are taken to be the minimizers of H with respect to $\langle s_4' \rangle$. Therefore, our assessment of stability of the ordered phases is as follows: *for each fixed temperature* $T^* > 0$, *find the minimum*,

$$\min_{\langle s_4' \rangle} H(\langle s_4' \rangle; T^*). \quad \text{(A6)}$$

Some local and global properties of the deflated free-energy H, especially *coerciveness*, have to be established in order to ensure the existence of such a minimum. Coerciveness ensures that the global minimum is to be found in a finite region of the domain of definition of H, and it coincides with a critical point. As a preliminary step we need to get information about the dependence of H on $\langle s_4' \rangle$ via the function Ξ. Taking into account that $\langle s_4'' \rangle = \Xi(\langle s_4' \rangle; T^*)$ we arrive at the following expression for the first derivative of Ξ (by direct calculation or as a consequence of the implicit function theorem):

$$\frac{d\Xi}{d\langle s_4' \rangle} = -\frac{\frac{\partial^2 E}{\partial \langle s_4' \rangle^2}}{\frac{\partial^2 E}{\partial \langle s_4' \rangle \partial \langle s_4'' \rangle}} = \frac{1}{36} \frac{\partial^2 E}{\partial \langle s_4' \rangle^2}, \quad \text{(A7)}$$

which holds at all points such that $\frac{\partial E}{\partial \langle s_4' \rangle} = 0$ [i.e., $\langle s_4'' \rangle = \Xi(\langle s_4' \rangle; T^*)$]. From Eq. (A4a) and from Eq. (A7) we learn that $\frac{d\Xi}{d\langle s_4' \rangle} < 0$ which means that Ξ is a strictly decreasing function of $\langle s_4' \rangle$. By also taking into account that $\Xi(0; T^*) = 0$ we conclude that $\langle s_4' \rangle \Xi(\langle s_4' \rangle; T^*) = \langle s_4' \rangle \langle s_4'' \rangle < 0$ whenever $\langle s_4' \rangle \neq 0$. We can now establish the above-mentioned coerciveness property of the deflated free-energy H, that is,

$$H(\langle s_4' \rangle; T^*) \to +\infty, \quad \text{as } |\langle s_4' \rangle| \to \infty \quad \forall T^*. \quad \text{(A8)}$$

Actually, in Eq. (A5), $s_5'(\omega_1), s_5''(\omega_2)$ are bounded and continuous functions and the integral is being calculated over a compact space (Euler angles); moreover the integrand in (A5) is dominated by the factor $\exp[72\beta \Xi(\langle s_4' \rangle; T^*) \langle s_4' \rangle]$ as $|\langle s_4' \rangle| \to \infty$. This stems from the fact that both $\langle s_4' \rangle \to \pm\infty$ and $\Xi(\langle s_4' \rangle; T^*) \to \mp\infty$ as $\langle s_4' \rangle \to \pm\infty$ while the other contributions in the integrand are linear in the order parameters. The dominant contribution in the integral of (A5) tends to zero in the same limit since $\langle s_4' \rangle \Xi(\langle s_4' \rangle; T^*) < 0$ and, in turn, the argument of ln in the same equation tends to vanish. We therefore arrive at (A8). As a consequence, H attains its global minimum at a critical point, and this point must be a least-free-energy point.

In fact more can be said about the criterion of stability (A6). It is possible to find the corresponding local stability criterion. Actually, the nature of the stationary points of H can be read off the sign of the second derivative of H. It turns out that

$$\frac{d^2 H}{d\langle s_4' \rangle^2} = \frac{\frac{\partial^2 E}{\partial \langle s_4' \rangle^2}}{\left(\frac{\partial^2 E}{\partial \langle s_4' \rangle \partial \langle s_4'' \rangle} \right)^2} \left[\frac{\partial^2 E}{\partial \langle s_4' \rangle^2} \frac{\partial^2 E}{\partial \langle s_4'' \rangle^2} - \left(\frac{\partial^2 E}{\partial \langle s_4' \rangle \partial \langle s_4'' \rangle} \right)^2 \right] = \frac{\frac{\partial^2 E}{\partial \langle s_4' \rangle^2}}{\left(\frac{\partial^2 E}{\partial \langle s_4' \rangle \partial \langle s_4'' \rangle} \right)^2} \det \mathbf{B}, \quad \text{(A9)}$$

where **B** is the Hessian matrix associated with E at its stationary points. Clearly the nature of the critical points of H is strictly connected with the nature of the corresponding points of E. The deflated free-energy H attains a minimum at the stationary point if $\det \mathbf{B} < 0$ so that $\frac{d^2H}{d\langle s_4' \rangle^2} > 0$, according to (A9) and (A4a). We thus conclude that the minimizers of H correspond actually to saddle points of E. Moreover, the stability of the phase can be read off the sign of one of the two eigenvalues of **B**. Actually, the two eigenvalues turn out to be

$$\Gamma_{\pm} = \frac{1}{2}\left[\mathrm{tr}\mathbf{B} \pm \sqrt{(\mathrm{tr}\mathbf{B})^2 - 4\det \mathbf{B}}\right], \tag{A10}$$

from which we conclude that $\Gamma_- < 0$. Accordingly, the stability of the phases is encoded in the sign of Γ_+.

As an example of the above outlined criterion, we consider the stability of the isotropic phase. To capture the bifurcation off the isotropic phase we compute the second derivative of H at $\langle s_4' \rangle = 0$ and we get

$$\frac{d^2H}{d\langle s_4' \rangle^2}(0; T^*) = 36\frac{9}{5T^*}\left[1 - \left(\frac{9}{5T^*}\right)^2\right], \tag{A11}$$

from which we conclude that the isotropic phase is stable for $T^* > \frac{9}{5}$. For $T^* < \frac{9}{5}$ the minimizer moves continuously from the isotropic phase and this latter becomes unstable. The actual migration of the minimizer close to the isotropic phase is provided by Eq. (34) and the corresponding least-free-energy value by Eq. (35).

We conclude this section by remarking that the same way of reasoning also applies to the MF approximation of KS as already worked out in [62].

[1] P. G. de Gennes, *The Physics of Liquid Crystals*, 1st ed. (Oxford University Press, Oxford, 1975).
[2] N. Chattham, E. Korblova, R. Shao, D. M. Walba, J. E. Maclennan, and N. A. Clark, Phys. Rev. Lett. **104**, 067801 (2010).
[3] G. Pelzl, S. Diele, and W. Weissflog, Adv. Mater. **11**, 707 (1999).
[4] B. Mettout, P. Tolédano, H. Takezoe, and J. Watanabe, Phys. Rev. E **66**, 031701 (2002).
[5] B. Mettout, Phys. Rev. E **72**, 031706 (2005).
[6] B. Mettout, Phys. Rev. E **74**, 041701 (2006).
[7] J. Matraszek, J. Mieczkowski, J. Szydłowska, and E. Gorecka, Liq. Cryst. **27**, 429 (2000).
[8] M. V. Jarić, Nucl. Phys. B **265**, 647 (1986).
[9] J. A. C. Veerman and D. Frenkel, Phys. Rev. A **45**, 5632 (1992).
[10] A. Chamoux and A. Pereira, J. Chem. Phys. **108**, 8172 (1998).
[11] R. Blaak, D. Frenkel, and B. M. Mulder, J. Chem. Phys. **110**, 11652 (1999).
[12] R. Blaak and B. M. Mulder, Phys. Rev. E **58**, 5873 (1998).
[13] B. S. John, A. Stroock, and F. A. Escobedo, J. Chem. Phys. **120**, 9383 (2004).
[14] B. S. John, A. Stroock, and F. A. Escobedo, J. Phys. Chem. B **109**, 23008 (2005).
[15] B. S. John, C. Juhlin, and F. A. Escobedo, J. Chem. Phys. **128**, 044909 (2008).
[16] R. D. Batten, F. H. Stillinger, and S. Torquato, Phys. Rev. E **81**, 061105 (2010).
[17] S. Romano, Phys. Rev. E **74**, 011704 (2006).
[18] M. J. Freiser, Phys. Rev. Lett. **24**, 1041 (1970).
[19] S. Romano, Physica A **337**, 505 (2004).
[20] G. De Matteis and S. Romano, Phys. Rev. E **78**, 021702 (2008).
[21] R. Berardi, L. Muccioli, S. Orlandi, M. Ricci, and C. Zannoni, J. Phys. Condens. Matter **20**, 463101 (2008).
[22] L. J. Yu and A. Saupe, Phys. Rev. Lett. **45**, 1000 (1980).
[23] G. R. Luckhurst, Thin Solid Films **393**, 40 (2001).
[24] V. Görtz, C. Southern, N. W. Roberts, H. F. Gleeson, and J. W. Goodby, Soft Matter **5**, 463 (2009).
[25] B. Senyuk, H. Wonderly, M. Mathews, Q. Li, S. V. Shiyanovskii, and O. D. Lavrentovich, Phys. Rev. E **82**, 041711 (2010).
[26] G. Cordoyiannis, D. Apreutesei, G. H. Mehl, C. Glorieux, and J. Thoen, Phys. Rev. E **78**, 011708 (2008).
[27] K. Neupane, S. W. Kang, S. Sharma, D. Carney, T. Meyer, G. H. Mehl, D. W. Allender, S. Kumar, and S. Sprunt, Phys. Rev. Lett. **97**, 207802 (2006).
[28] C. D. Southern, P. D. Brimicombe, S. D. Siemianowski, S. Jaradat, V. Roberts, V. Görtz, J. W. Goodby, and H. F. Gleeson, Europhys. Lett. **82**, 56001 (2008).
[29] G. R. Luckhurst, Angew. Chem., Int. Ed. **44**, 2834 (2005).
[30] G. R. Luckhurst, Liq. Cryst. **36**, 1295 (2009).
[31] R. Y. Dong, Int. J. Mod. Phys. B **24**, 4641 (2011).
[32] A. G. Vanakaras and D. J. Photinos, J. Chem. Phys. **128**, 154512 (2008).
[33] S. D. Peroukidis, P. K. Karahaliou, A. G. Vanakaras, and D. J. Photinos, Liq. Cryst. **36**, 727 (2009).
[34] O. Francescangeli, F. Vita, C. Ferrero, T. Dingemans, and E. T. Samulsky, Soft Matter **7**, 895 (2011).
[35] P. K. Karahaliou, A. G. Vanakaras, and D. J. Photinos, J. Chem. Phys. **131**, 124516 (2009).
[36] M. V. Gorkunov, M. A. Osipov, A. Kocot, and J. K. Vij, Phys. Rev. E **81**, 061702 (2010).
[37] M. A. Osipov and M. V. Gorkunov, J. Phys. Condens. Matter **22**, 362101 (2010).
[38] J. L. Figuerinhas, G. Feio, C. Cruz, M. Lehmann, C. Köhn, and R. Y. Dong, J. Chem. Phys. **133**, 174509 (2010).
[39] G. R. Luckhurst, Nature (London) **430**, 413 (2004).
[40] G. R. Luckhurst, British Liquid Crystal Society Newsletter, August, 10, 2005 [http://www-g.eng.cam.ac.uk/blcs/].
[41] J.-H. Lee, T.-K. Lim, W.-T. Kim, and J. I. Jin, J. Appl. Phys. **101**, 034105 (2007).
[42] R. Berardi, L. Muccioli, and C. Zannoni, J. Chem. Phys. **128**, 024905 (2008).
[43] M. Nagaraj, K. Merkel, J. K. Vij, and A. Kocot, Europhys. Lett. **91**, 66002 (2010).
[44] L. M. Blinov, Liq. Cryst. **24**, 143 (1998).
[45] O. Francescangeli *et al.*, Adv. Funct. Mater. **19**, 2592 (2009).
[46] A. M. Sonnet, E. G. Virga, and G. E. Durand, Phys. Rev. E **67**, 061701 (2003).

[47] G. De Matteis and E. G. Virga, Phys. Rev. E **71**, 061703 (2005).
[48] F. Bisi, E. G. Virga, E. C. Gartland Jr., G. De Matteis, A. M. Sonnet, and G. E. Durand, Phys. Rev. E **73**, 051709 (2006).
[49] R. Rosso and E. G. Virga, Phys. Rev. E **74**, 021712 (2006).
[50] G. De Matteis, F. Bisi, and E. G. Virga, Continuum Mech. Thermodyn. **19**, 1 (2007).
[51] E. C. Gartland Jr. and E. G. Virga, Arch. Ration. Mech. Anal. **196**, 143 (2010).
[52] S. Romano, Phys. Lett. A **333**, 110 (2004).
[53] G. De Matteis, S. Romano, and E. G. Virga, Phys. Rev. E **72**, 041706 (2005).
[54] Z.-D. Zhang, Y.-J. Zhang, and Z.-L. Sun, Chin. Phys. Lett. **23**, 3025 (2006).
[55] D. Allender and L. Longa, Phys. Rev. E **78**, 011704 (2008).
[56] P. K. Mukherjee and K. Sen, J. Chem. Phys. **130**, 141101 (2009).
[57] G. De Matteis, A. M. Sonnet, and E. G. Virga, Continuum Mech. Thermodyn. **20**, 347 (2008).
[58] G. De Matteis and S. Romano, Phys. Rev. E **80**, 031702 (2009).
[59] G. Lasher, Phys. Rev. A **5**, 1350 (1972).
[60] P. Pasini, C. Chiccoli, and C. Zannoni, *Advances in the Computer Simulations of Liquid Crystals*, edited by P. Pasini and C. Zannoni, Vol. 545 of NATO Science Series C (Kluwer, Dordrecht, 2000), Chap. 5.
[61] G. Kohring and E. Shrock, Nucl. Phys. B **295**, 36 (1988).
[62] S. Romano, Int. J. Mod. Phys. B **8**, 3389 (1994).
[63] H. G. Ballesteros, L. A. Fernández, V. Martín-Mayor, and A. Munõz-Sudupe, Phys. Lett. B **378**, 207 (1996); Nucl. Phys. B, Proc. Suppl. **53**, 686 (1997); Nucl. Phys. B **483**, 707 (1997).
[64] C. Zannoni, in *The Molecular Physics of Liquid Crystals*, edited by G. R. Luckhurst and G. W. Gray (Academic Press, London, 1979), Chaps. 3 and 9.
[65] C. Chiccoli, P. Pasini, F. Biscarini, and C. Zannoni, Mol. Phys. **65**, 1505 (1988).
[66] C. Zannoni, in *Advances in the Computer Simulations of Liquid Crystals*, edited by P. Pasini and C. Zannoni, Vol. 545 of NATO Science Series C (Kluwer, Dordrecht, 2000), Chap. 2.
[67] G. J. Villain, R. Bidaux, J.-P. Carton, and R. Conte, J. Phys. (Paris) **41**, 1263 (1980).
[68] S. Prakash and C. L. Henley, Phys. Rev. B **42**, 6574 (1990).
[69] M. Biskup, L. Chayes, and S. A. Kivelson, Ann. Henri Poincaré **5**, 1181 (2004).
[70] C. Chiccoli, P. Pasini, F. Semeria, and C. Zannoni, Int. J. Mod. Phys. C **10**, 469 (1999).
[71] D. M. Brink and G. R. Satchler, *Angular Momentum*, 2nd ed. (Oxford University Press, Oxford, 1968).
[72] D. A. Varshalovich, A. N. Moskalev, and V. K. Khersonskii, *Quantum Theory of Angular Momentum* (World Scientific, Singapore, 1988).
[73] G. B. Arfken and H. J. Weber, *Mathematical Methods for Physicists*, 4th ed. (Academic Press, San Diego, 1995).
[74] J. P. Straley, Phys. Rev. A **10**, 1881 (1974).
[75] G. R. Luckhurst, C. Zannoni, P. L. Nordio, and U. Segre, Mol. Phys. **30**, 1345 (1975).
[76] F. Biscarini, C. Chiccoli, P. Pasini, F. Semeria, and C. Zannoni, Phys. Rev. Lett. **75**, 1803 (1995).
[77] B. Mulder, Phys. Rev. A **39**, 360 (1989).
[78] R. Rosso, Liq. Cryst. **34**, 737 (2007).
[79] G. R. Luckhurst and S. Romano, Mol. Phys. **40**, 129 (1980).
[80] B. Bergersen, P. Palffy-Muhoray, and D. A. Dunmur, Liq. Cryst. **3**, 347 (1988).
[81] L. Longa, P. Grzybowski, S. Romano, and E. Virga, Phys. Rev. E **71**, 051714 (2005); **73**, 019904E (2006).
[82] L. Longa and G. Pajak, Liq. Cryst. **32**, 1409 (2005).
[83] F. Bisi, S. Romano, and E. G. Virga, Phys. Rev. E **75**, 041705 (2007).
[84] F. Bisi, G. R. Luckhurst, and E. G. Virga, Phys. Rev. E **78**, 021710 (2008).
[85] A. M. Sonnet and E. G. Virga, Phys. Rev. E **77**, 031704 (2008).
[86] F. Y. Wu, Rev. Mod. Phys. **54**, 235 (1982).
[87] J.-S. Wang, R. H. Swendsen, and R. Kotecký, Phys. Rev. B **42**, 2465 (1990).
[88] A. P. Gottlob and M. Hasenbusch, Physica A **210**, 217 (1994).
[89] S. Rahman, E. Rush, and R. H. Swendsen, Phys. Rev. B **58**, 9125 (1998).
[90] C. Yamaguchi and Y. Okabe, J. Phys. A **34**, 8781 (2001).
[91] M. Golubitsky and D. G. Schaeffer, *Singularities and Groups in Bifurcation Theory*, Vol. I (Springer, New York, 1985).
[92] R. Hashim and S. Romano, Int. J. Mod. Phys. B **13**, 3879 (1999).
[93] G. R. Luckhurst, in *Physical Properties of Liquid Crystals: Nematics*, edited by D. A. Dunmur, A. Fukuda, and G. R. Luckhurst (INSPEC, London, 2001), Chap. 2.1.
[94] M. P. Allen, Liq. Cryst. **8**, 499 (1990).
[95] R. J. Low, Eur. J. Phys. **23**, 111 (2002).
[96] S. Romano, Phys. Rev. E **77**, 021704 (2008).